Animal Model

Optical Imaging of Cancer Metastasis to Bone Marrow

A Mouse Model of Minimal Residual Disease

Antoinette Wetterwald,* Gabri van der Pluijm,†
Ivo Que,† Bianca Sijmons,† Jeroen Buijs,†
Marcel Karperien,† Clemens W. G. M. Löwik,†
Elsbeth Gautschi,* George N. Thalmann,* and
Marco G. Cecchini*

*From the Department of Clinical Research and Department of
Urology,* Gene Therapy Laboratory, University of Bern,
Inselspital, Bern, Switzerland; and the Department of
Endocrinology,† Leiden University Medical Centre, Leiden,
The Netherlands*

The development of novel anti-cancer strategies requires more sensitive and less invasive methods to detect and monitor *in vivo* minimal residual disease in cancer models. Bone marrow metastases are indirectly detected by radiography as osteolytic and/or osteosclerotic lesions. Marrow micrometastases elude radiographic detection and, therefore, more sensitive methods are needed for their direct identification. Injection of cancer cells into the left cardiac ventricle of mice closely mimics micrometastatic spread. When luciferase-transfected cells are used, whole-body bioluminescent reporter imaging can detect microscopic bone marrow metastases of ≈ 0.5 mm^3 volume, a size below the limit in which tumors need to induce angiogenesis for further growth. This sensitivity translates into early detection of intramedullary tumor growth, preceding the appearance of a radiologically evident osteolysis by ≈ 2 weeks. Bioluminescent reporter imaging also enables continuous monitoring in the same animal of growth kinetics for each metastatic site and guides end-point analyses specifically to the bones affected by metastatic growth. This model will accelerate the understanding of the molecular events in metastasis and the evaluation of novel therapies aiming at repressing initial stages of metastatic growth. *(Am J Pathol 2002, 160:1143–1153)*

Because of the progress made in early detection and surgical treatment of the primary tumor, mortality in cancer patients is increasingly linked to metastatic disease. Bone is the second most common site of metastasis[1] and the frequency of bone metastases at autopsy of cancer patients varies between 60% and 85%, depending on the cancer type.[2–4]

Clinical and experimental observations indicate that the hematopoietic marrow, rather than the bone tissue, is the initial site of cancer cell seeding.[5] Indeed, small clusters of cancer cells (micrometastases) can be detected in a vast proportion of the bone marrow aspirates of patients affected by a variety of epithelial cancers with no radiological or scintigraphic evidence of bone metastasis at the time of diagnosis and/or surgery of the primary tumor.[6,7] Micrometastases represent the pathophysiological basis of minimal residual disease[8,9] that will eventually lead to cancer relapse as overt metastases. However, they cannot be detected by conventional staging methods and are poorly influenced by current treatment.[8–10] Hence, there is a need for alternative therapeutic strategies that should be tested in experimental models able to mimic micrometastatic spread.

Injection of cancer cell lines into the left cardiac ventricle of immunodeficient (*nu/nu*) mice is a widely used animal model of bone/bone marrow metastasis.[11,12] This experimental setting closely resembles the clinical situation of minimal residual disease after removal of the primary tumor. However, detection of bone metastasis by radiography[13] makes it not an ideal model of minimal residual disease. In fact, radiologically evident osteolytic/

osteosclerotic metastases are a late and macroscopic event in the evolution of metastatic bone disease. Thus, the model lacks the sensitivity that would be necessary to dissect the initial processes, such as the "angiogenic switch,"[14] essential for tumor progression.[15] Furthermore, the radiological detection of osteolytic and/or osteosclerotic metastases is an indirect measure of the tumor burden. Only a parallel histomorphometric analysis allows the distinction between a therapeutic effect exerted directly on tumor cells or indirectly through inhibition of bone resorption. Therefore, more sensitive methods to detect and monitor directly metastatic growth in bone marrow/bone of whole animals need to be developed.

Expression *in vivo* of reporter genes encoding bioluminescent[16] or fluorescent[17] proteins can be detected externally by sensitive detection systems. Cancer cell lines permanently transfected either with the firefly luciferase (*Luc*) or the green fluorescent protein (GFP) have been used to monitor in living mice local tumor growth[18] and development of metastasis to different organs.[17]

We investigated the possibility of applying an equivalent bioluminescent imaging method to visualize *in vivo* the development of bone marrow/bone metastases after injection of luciferase-transfected MDA-MB-231 cells, a human mammary carcinoma cell line,[19] into the left cardiac ventricle of immunodeficient (*nu/nu*) mice.

Here we demonstrate that whole-body bioluminescent reporter imaging (BRI) effectively allows sensitive localization and growth monitoring of minimal metastatic deposits in the bone marrow at a stage largely preceding tumor-induced osteolysis.

Materials and Methods

Animals

Female BALB/c *nu/nu* mice were purchased from Iffa Credo (L'Arbresle, France). They were housed in individual ventilated cages under sterile conditions according to the Swiss guidelines for the care and use of laboratory animals. Sterile food and water were provided *ad libitum*. Mice were 5 to 6 weeks old when used for the intracardiac injection of tumor cells. For intraosseous, intramuscle, and subcutaneous implantation of tumor cells they were 10 to 12 weeks old.

For surgical manipulation, mice were anesthetized by an intraperitoneal injection of a mixture of Domitor (1 mg/kg body weight; Pfizer, Sandwich, UK), Climasol (10 mg/kg body weight; Gräub, Bern, Switzerland), and Fentanyl (100 μg/kg body weight; University of Bern Hospital pharmacy). Mice were recovered from anesthesia by a subcutaneous injection of a mixture of the following antidotes: Antisedan (5 mg/kg body weight; Pfizer), Sarmasol (1 mg/kg body weight; Gräub), and Narcan (2.4 mg/kg body weight; Dupont Pharma, Wilmington, DE).

Mice subjected to intracardiac injection of tumor cells were sacrificed by CO_2 euthanasia at first signs of distress and/or paraplegia. Mice injected subcutaneously, intramuscularly, and/or intraosseously with tumor cells were sacrificed immediately after BRI analysis, and those with tumor cells implanted intraosseously were sacrificed at the end of the 5-week observation period.

Cell Lines

The human mammary carcinoma cell line MDA-MB-231 (MDA-231) was obtained from the American Type Culture Collection (Rockville, MD). A subclone inducing invariably bone metastases after intracardiac inoculation (bone-seeking clone, MDA-231-B) has been established by sequential cycles of intracardiac inoculation of MDA-231 *in vivo* and expansion *in vitro* of the cell population recovered from the resulting bone metastases. Briefly, parental MDA-231 cells [1×10^5/100 μl phosphate-buffered saline (PBS)] were injected intracardiac in female BALB-c *nu/nu* mice. Development of osteolytic bone metastases was monitored by radiography. When the bone metastases reached the size of ≈2-mm diameter, they were dissected out, cut into small fragments, and transferred to 12-well plates. After 3 days of culture, remnants of the original tissue fragments were removed and each area of cell outgrowth was individually trypsinized with the aid of cloning rings. The individual cell populations resulting from each area of outgrowth were separately expanded by limiting dilution. After expansion, the origin of the clones from the cancer cell population of the original metastases was confirmed by species-specific polymerase chain reaction analysis for human β2-microglobulin, as described earlier.[20] Positive clones only were selected for a new cycle of intracardiac inoculation *in vivo* and expansion *in vitro* of the cell population recovered from the resulting bone metastases. The MDA-231-B subclone was obtained after a total of four of these consecutive cycles. It showed the capacity, after intracardiac inoculation, to induce bone metastases, as detected by radiography, in 100% of the animals. For this reason it was selected for the establishment of stable transfectants expressing the luciferase gene.

Cell lines and the explanted fragments of bone metastases were grown in Dulbecco's modified Eagle's medium (Biochrom, Basel, Switzerland) containing 4.5 g of glucose/L and supplemented with 10% newborn calf serum (Biowhittaker, Verviers, Belgium) and 1% gentamicin. Cells were regularly certified free of mycoplasma contamination.

Establishment of Stable Transfectants Expressing the Luciferase Reporter Gene

A CMV promoter-driven mammalian expression vector for luciferase (CMV-Luc) was generated by cloning a full-length firefly luciferase cDNA[21] into the pcDNA3.1 plasmid (Invitrogen, Breda, Netherlands). MDA-231-B cells were transfected with 1 μg of CMV-Luc using fugene-6 (Roche Biochemicals, Almere, The Netherlands). Stable transfectants were selected with G418 (800 μg/ml; Life Technologies, Basel, Switzerland). Twenty-five different G418-resistant clones were isolated, subcloned, and tested for luciferase activity. Six clones were found to express luciferase activity. One clone (MDA-231-B/

Luc+), expressing the highest levels of luciferase activity (5 to 12 RLU/μg cell protein) was selected for further experimentation. The clone has been cultured up to 40 passages and, even though in some passages the cells have been propagated in absence of G418 selection, the clone maintains currently the same level of luciferase expression of early passages.

Induction of Metastases by Intracardiac and Intravenous Injection of Cancer Cells

A single cell suspension of MDA-231-B/*Luc*+ cells (1 × 10^5/100 μl PBS) was injected into the left heart ventricle according to the method described by Arguello and co-workers.[11] Some animals were injected into the tail vein with an equal number of MDA-231-B/*Luc*+ cells. The development of metastases was monitored weekly by BRI and radiography. Some of the mice were also imaged 10 minutes and 24 hours after intracardiac injection to visualize the early body distribution of MDA-231-B/*Luc*+ cells.

Intraosseous Implantation of Cancer Cells

For direct intraosseous implantation of MDA-231-B/*Luc*+ cells, two holes, 4 to 5 mm distant from each other and each with a diameter of ~0.35 mm, were drilled through the bone cortex of the upper third of the right tibia with the aid of a dental drill (Hedstroem file, 28 mm/30; Maillefer Instruments, Ballaigues, Switzerland). Space in the marrow cavity was created by flushing out the bone marrow of the proximal segment of the bone shaft. The upper hole was sealed by surgical bone wax (Ethicon; Johnson and Johnson, Somerville, NJ) and a single cell suspension of MDA-231-/*Luc*+ cells (1 × 10^4/2 μl of PBS) slowly inoculated via a 30-gauge needle inserted through the lower hole. Finally, the lower hole was sealed with surgical bone wax and the cutaneous wound was sutured. Local tumor development was monitored twice a week by BRI and radiography. This method was adopted to prevent spill of cancer cells from the channel created by the needle and subsequent growth outside the marrow cavity into the surrounding soft tissues during the following period (28 days) of monitoring.

Determination of the Lowest Cell Number Detectable in Bone

The knee articulation was forced in a flexed position and a 27-gauge needle was inserted through the patellar tendon and guided toward the articular surface of the femur with gentle drilling motion until the bone cortex was perforated.[22] Ten thousand to 1 million MDA-231-B/*Luc*+ cells in a total volume of 5 μl of PBS were slowly injected into the bone marrow cavity. As control, 1 × 10^4 cells were injected intramuscularly, in the vastus lateralis. As further control, 1 × 10^1, 1 × 10^2, 1 × 10^3, and 1 × 10^4 cells were injected subcutaneously, in the ventral region. A single BRI analysis was performed after 15 minutes.

The choice of this less invasive and faster method of cell inoculation was essentially dictated by the necessity to detect bioluminescent emission immediately after cell implantation and by the fact that in this case spill of cancer cells into the soft tissue was less an issue because tumor growth was not followed-up.

Bioluminescent Reporter Imaging (BRI)

An imaging system essentially equivalent to that described by Edinger and co-workers[18] was used. The imaging unit consists of an intensified charge-coupled device camera (VIM camera, model C2400-47; Hamamatsu Photonics, Hamamatsu, Japan) fitted to a light-tight chamber (Hamamatsu Photonics) and equipped with a 50 mm/f 1.2 Nikkor lens (Nikon, Küsnacht, Switzerland). The images are generated on an Argus-20 image processor (Hamamatsu Photonics) and transferred via SCSI using a software module (Openlab; Improvision, Coventry, UK) to a computer (Macintosh G4; Apple Computer, Cupertino, CA) and processed by image analysis software (Openlab; Improvision, Coventry, UK).

For the detection of luciferase-expressing cells, mice were anesthetized as described above, but using half the doses of each sedative. Thirty μl of a 250-mmol/L aqueous solution of luciferin (D-luciferin Na salt; Molecular Probes, Leiden, The Netherlands) were injected intraperitoneally 15 minutes before beginning photon recording. Mice were placed in the light-tight chamber and a gray-scale image of the animal was first recorded with dimmed light. Photon emission was then integrated throughout a period of 5 minutes and recorded as pseudo-color images. For co-localization of the bioluminescent photon emission on the animal body, gray-scale and pseudo-color images were merged by using the Openlab imaging software.

Quantification of the Bioluminescent Signal

The bioluminescent signal was quantified by measuring the amount of highlighted pixels in the area shaped around each site of photon emission with the aid of the Openlab imaging software.

Detection of Bone Lesions by Radiography

Radiographs of the mice, anesthetized as described above for the BRI analysis, were taken using X-Omat TL films (Kodak, Lausanne, Switzerland).

Immunohistochemistry

The mice injected with intracardiac MDA-231-B/Luc+ cells were perfused, after sacrifice, with 60 ml of Hanks' balanced salt solution containing 20 U heparin/ml and, then, with 100 ml of 4% paraformaldehyde in Dulbecco's PBS, pH 7.4. Bones that were shown by BRI to be the site of bioluminescent emission were selectively excised and further fixed overnight by immersion in fixative at 4°C.
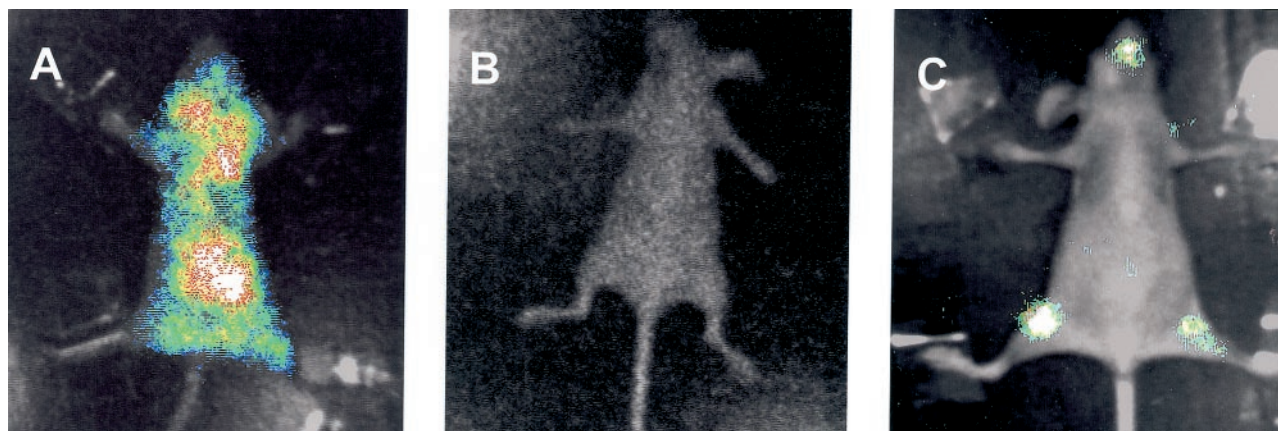
Figure 1. Fate of MDA-231-B/*Luc*+ cells injected into the left cardiac ventricle. Bioluminescent photon emission was externally imaged from the ventral projection of the same mouse 10 minutes (**A**), 24 hours (**B**), and 28 days (**C**) after injection. Signals are displayed as pseudo-color image (blue least intense, white most intense) at a 0- to 4-bit sensitivity range merged with the gray-scale body image of the mouse.

After decalcification in ethylenediaminetetraacetic acid they were processed for paraffin embedding.

Five-μm serial sections, after rehydration and endogenous peroxidase block, were digested for 20 minutes at 37°C with trypsin (0.1% in 25 mmol/L Tris, 140 mmol/L NaCl, and 10 mmol/L CaCl$_2$) for antigen retrieval. Rabbit antibodies (10 μg/ml) against human pan-cytokeratin (DAKO, Zug, Switzerland) or control normal rabbit IgG (Jackson ImmunoResearch, La Roche, Switzerland) were followed by biotinylated swine anti-rabbit Ig antibodies (DAKO) and streptavidin-biotinylated peroxidase complex (Amersham, Dubendorf, Switzerland). The reaction was developed with 3-amino-9-ethyl-carbazole as chromogen. Sections were slightly counterstained with hematoxylin. Size measurements of metastatic lesions were performed with the aid of image analysis software (NIH Image; *http://rsb.info.nih.gov/nih-image*).

Results

Monitoring in Vivo Development of Metastases after Intracardiac and Intravenous Injection of Cancer Cells

In general, within 2 hours from the intracardiac injection of MDA-231-B/*Luc*+ cells 14% of the mice died or showed signs of distress, for which they were subjected to euthanasia. The surviving mice all developed bone metastases as detected by BRI. In contrast, none of the mice ($n = 4$) injected intravenously showed either bone or soft tissue metastases during the entire period of observation (4 weeks), as detected both by BRI and radiography.

Ten minutes after intracardiac injection of MDA-231-B/*Luc*+ cells, BRI showed diffuse photon accumulation over the entire animal body, with exclusion of the distal forelegs and hindlegs, and of the tail (Figure 1A). Twenty-four hours later photon emission from the same animal was abolished (Figure 1B). However, after 4 weeks BRI could detect distinct areas of photon accumulation, suggestive of metastatic tumor growth, over the hind-

legs and over the maxillofacial region of the same animal (Figure 1C).

The first evidence of bioluminescent emission from bones, indicative of bone metastasis, was seen at day 24 after intracardiac injection of cancer cells. In all mice ($n = 4$) discrete photon accumulation was localized over the distal metaphyses of the femurs (Figure 2; A to D) and over the dorsal projection of the thoracic vertebrae (not shown). In one mouse photons accumulated also over the proximal metaphysis of the tibia (Figure 2B). Whole body radiographs taken at day 25 did not show any sign of osteolysis in any of the bones and, more specifically, in any of the bone locations that were the origin of photon emission recorded the previous day (not shown).

The intensity of photon emission at the bone sites described above increased substantially from day 24 to day 33. Furthermore, at day 33, additional bone sites of bioluminescence became apparent (Figure 3; A to F). At this time point, the average number of bone metastasis/mouse attained to 6.33 ($\pm$1.45, SEM). However, whole body radiographs taken at the same day showed bone lesions only in one-third of the bone sites revealed by photon detection (total 19 *versus* 6 bone sites, as detected by BRI and radiography, respectively; n mice = 3) (not shown). One animal survived until day 38 after intracardiac injection of cancer cells. In this mouse an additional bioluminescent site appeared in the region of the sacral vertebrae (Figure 4B). Meanwhile, the signal intensity over all of the other bone sites further increased (Figure 4; A to C), as compared to day 33. However, the radiographic analysis of the bone lesions at day 38 did not reveal a modification in their number (Figure 4D), as compared to day 33. In all cases the bone lesions were characterized by subtle modifications of the metaphyseal spongiosa because of increased bone remodeling and/or limited areas of osteolysis (Figure 4, E and F). At any time point, none of the animals of this series showed photon emission at extra-skeletal locations.

The quantification of the bioluminescent signal localized over the different bone metastatic sites from the time of their first appearance to the time of animal sacrifice
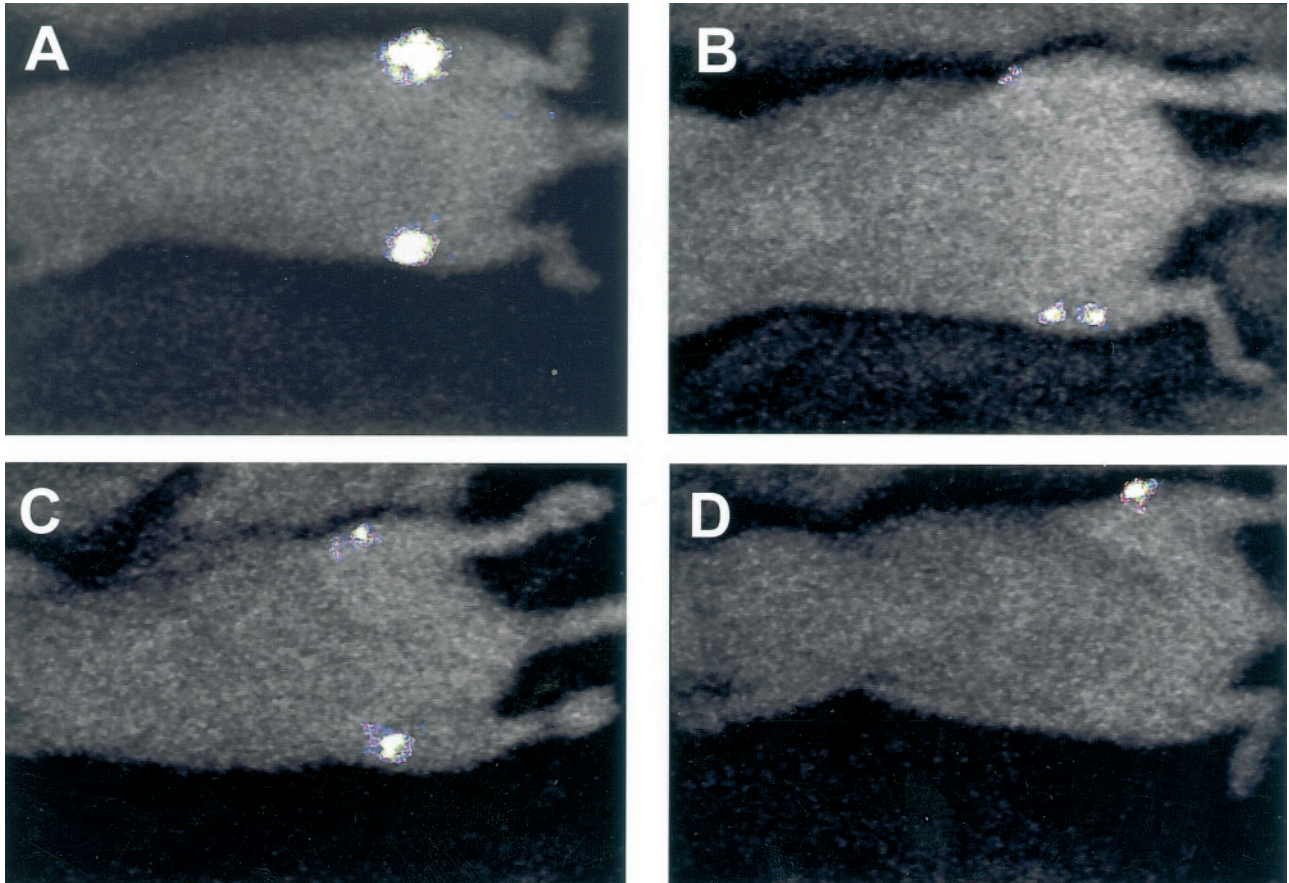
Figure 2. BRI monitoring *in vivo* of the kinetics of bone metastatic growth. Bioluminescent photon emission was externally imaged 24 days after injection of MDA-231-B/*Luc*+ cells into the left cardiac ventricle. **A–D:** Ventral projections of four different mice. Signals are displayed as pseudo-color image at the most sensitive 0- to 3-bit range.

(Figure 4G) allowed continuous monitoring *in vivo* of the growth kinetics for each single bone lesion.

Immunohistochemical analysis for human pan-cytokeratin expression confirmed the presence of cancer cells in all of the bones that were shown by BRI to be the site of bioluminescent emission. One bone metastatic growth was identified both by BRI and radiography as located in the proximal metaphysis of the humerus (Figure 4, A and D). The histological and immunohistological analyses showed that cancer cells have extensively invaded the proximal half of the bone marrow cavity of this bone (Figure 5, A and C). In contrast, small bone metastases were apparently located by BRI on the distal region of both tibiae (Figure 3, D and F, and Figure 4; A to C), but their presence was not corroborated by radiological signs of increased bone turnover located in the same or in neighboring bones. However, the histological and immunohistochemical analysis of the bones in this region revealed that a single metastatic focus was located in the epiphysis of each calcaneus bone (Figure 5, B and D).

MDA-231-B/*Luc*+ cells were intracardiac injected in another series of mice ($n = 12$) to further investigate the potential of this specific bone-seeking clone to metastasize to organs other than bone and to demonstrate the ability of BRI to detect development of soft tissue metastasis. Bone metastases developed in 100% of the mice

(12 of 12; average number of bone metastases/mouse: 5.33 ± 0.78 SEM). Soft tissue metastases were detected by BRI in 33% of the mice (4 of 12; average number of soft tissue metastases/mouse: 0.33 ± 0.14 SEM). Lung and brain were the organs affected by the metastatic process in 25% (3 of 12) and 8% (1 of 12), respectively, of the mice injected.

During the entire experimental period in both series of intracardiac inoculated mice none of the bone metastases detected by BRI showed a decline in bioluminescent activity. Furthermore, conventional radiography never detected an osteolytic lesion not showing bioluminescent emission.

Monitoring in Vivo *Tumor Growth after Intraosseous Implantation of Cancer Cells*

Soon after implantation of 1×10^4 MDA-231-B/*Luc*+ cells into the tibia marrow cavity, no bioluminescent emission could be detected externally. However, already after 4 days there was a defined, although weak, photon emission localized over the area of implant. The signal on the same area increased progressively and became intense from day 14 (Figure 6A). Nevertheless, radiographs taken at equivalent time points (Figure 6B) showed initial signs
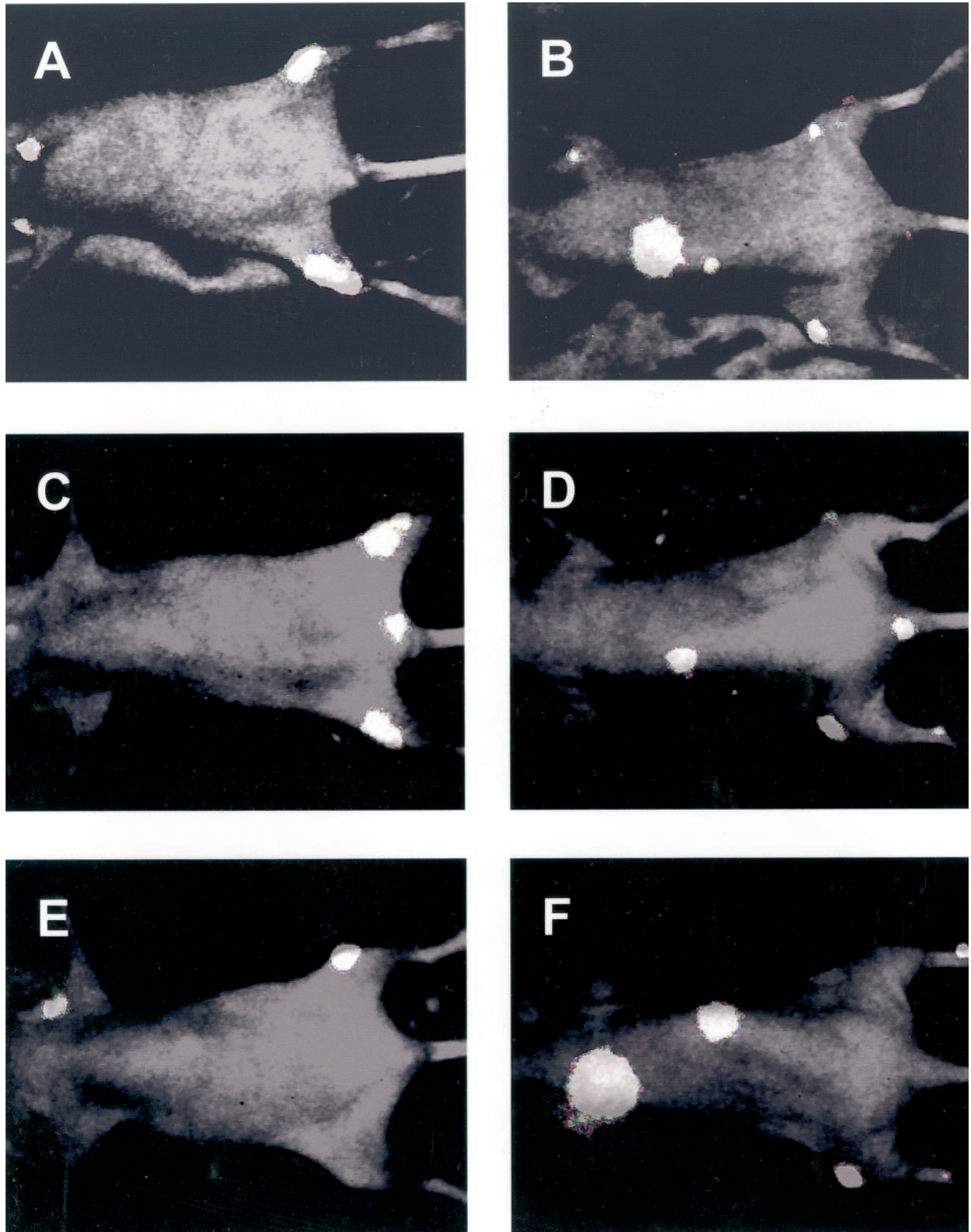
Figure 3. BRI monitoring *in vivo* of the kinetics of bone metastatic growth. Bioluminescent photon emission was externally imaged 33 days after injection of MDA-231-B/*Luc*+ cells into the left cardiac ventricle. Ventral (**A**, **C**, **E**) and dorsal (**B**, **D**, **F**) projections of the three mice shown in Figure 2; B, C, and D, respectively. Signals are displayed as pseudo-color image at a 0- to 5-bit range, less sensitive than that of Figure 2, to optimize the anatomical localization.
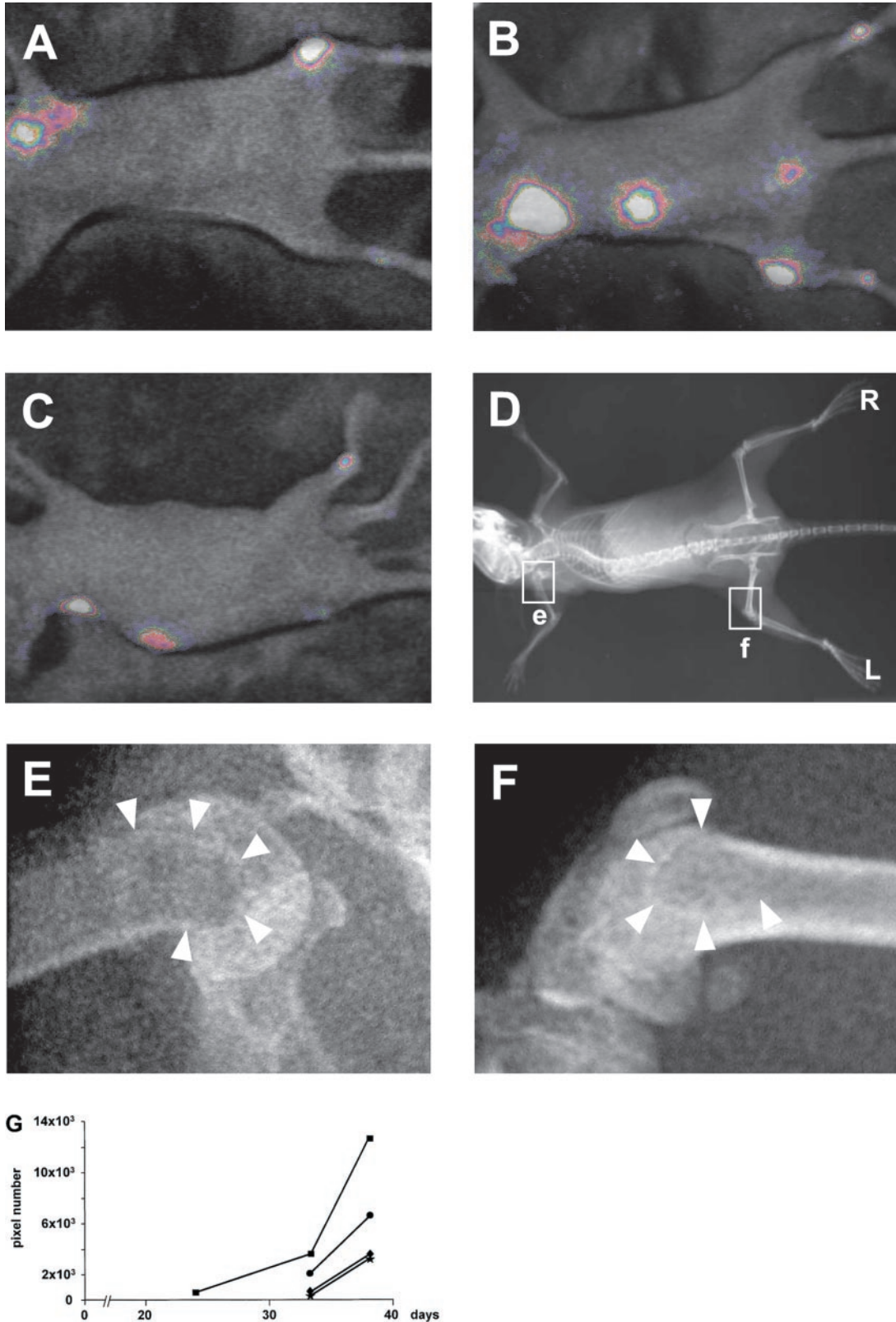
Figure 4. BRI and radiographic monitoring *in vivo* of the kinetics of bone metastatic growth. Bioluminescent photon emission was externally imaged 38 days after injection of MDA-231-B/*Luc*+ cells into the left cardiac ventricle. Ventral (**A**), dorsal (**B**), and lateral (**C**) projections of the mouse shown in Figure 3, E and F. Signals are displayed as pseudo-color image at a 0- to 6-bit range, less sensitive than that of Figure 4, to optimize anatomical localization. **D:** Whole body radiograph. R, right side; and L, left side of the mouse. The two regions delimited by the rectangular frames on the proximal humerus (e) and on the distal femur (f) are magnified in **E** and **F**, respectively, showing details of the bone density. **Arrowheads** point at osteosclerotic rims delineating areas of discrete osteolysis. **G:** Growth curve obtained by quantification in the same mouse of the bioluminescent signal localized over the left femur (■) at day 24, as shown in Figure 2D, and over the central portion of the spine (●) and the distal regions of the right (♦) and left (★) tibia at day 33, as shown in Figure 3, E and F, and at day 38 (**A** and **B**).
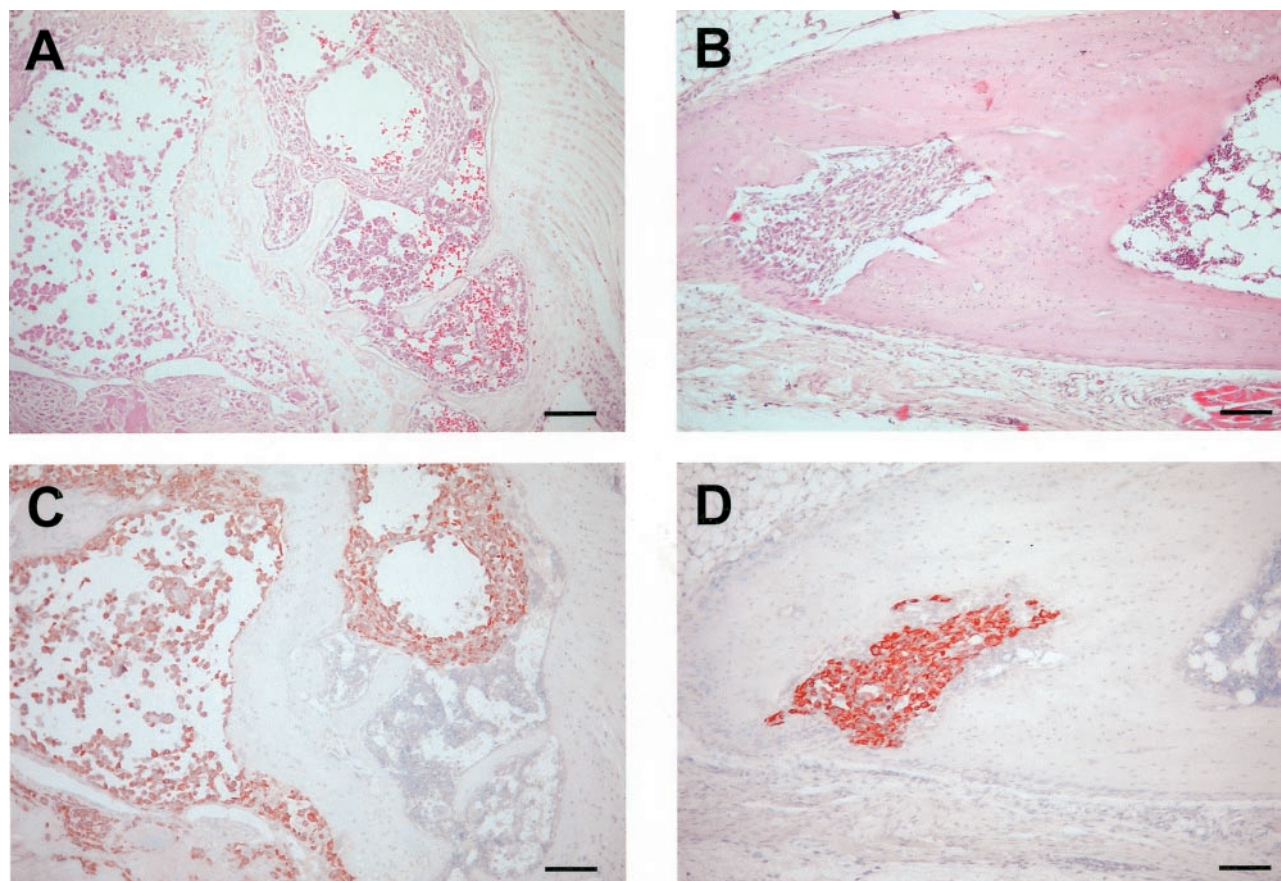
Figure 5. Histological and immunohistological identification of MDA-231-B/*Luc+* cells in two representative sites of metastasis. H&E staining of sections from the left humerus (**A**) and the left calcaneus (**B**). Cytokeratin immunohistochemistry of adjacent sections from **C**, the same humerus, and **D**, the calcaneus. Cells immunoreactive with the anti-human pan-cytokeratin antibody are stained in brownish-red. Scale bars, 100 μm.

of osteolysis only at day 14. The osteolysis in the trabecular bone became clearly evident at day 25, and substantial erosion of the cortical bone was obvious at day 36.

The quantification at different time points of the bioluminescent signal localized over the site of implantation (Figure 6C) allowed continuous monitoring *in vivo* of tumor growth.

### Determination of the Lowest Cell Number Detectable in Bone by BRI

Soon after direct inoculation of MDA-231-B/*Luc+* cells into the marrow cavity of the femur, BRI could detect a signal from a number of cells as low as 2×10^4. However, 1×10^4 and 0.1×10^4 cells could be detected if injected intramuscularly and subcutaneously, respectively (not shown). Similarly, microscopic foci of spontaneous bone metastasis could easily be detected. In the specific case shown in Figure 5, B and D, the three major diameters of the metastatic lesion and the density of the cancer cells were determined in serial sections comprehensive of the entire extension of the metastatic lesion. Assuming an ellipsoid shape, the total volume of the metastatic lesion resulted of $\sim$0.5-mm^3 volume and the total number of cells contained in it was calculated as $\sim$1.7 $\times$ 10^4.

Discussion

This investigation shows for the first time that the intracardiac injection of MDA-231-B/*Luc+* cancer cells combined to BRI is an ideal model for minimal residual disease because of the remarkable sensitivity of the optical imaging in detecting microscopic bone marrow metastases *in vivo*.

The fate of the MDA-231-B/*Luc+* cells could already be monitored by BRI immediately after intracardiac injection. The diffuse photon signal imaged over the entire animal body 10 minutes after injection was likely to be emitted by cancer cells not yet extravasated, and the areas of denser emission reflected presumably organs with the highest blood flow. The absence of signal 24 hours later conforms to the already reported rapid clearance and elimination of the majority of intracardiac-injected cancer cells.[23] Consistently with the elective bone/bone marrow tropism of the parental clone MDA-231-B, the same animal developed exclusively bone metastases within 4 weeks from intracardiac injection of MDA-231-B/*Luc+* cells. These findings further support the concept that organ specificity of metastases is not because of differences in blood perfusion, but primarily depends on
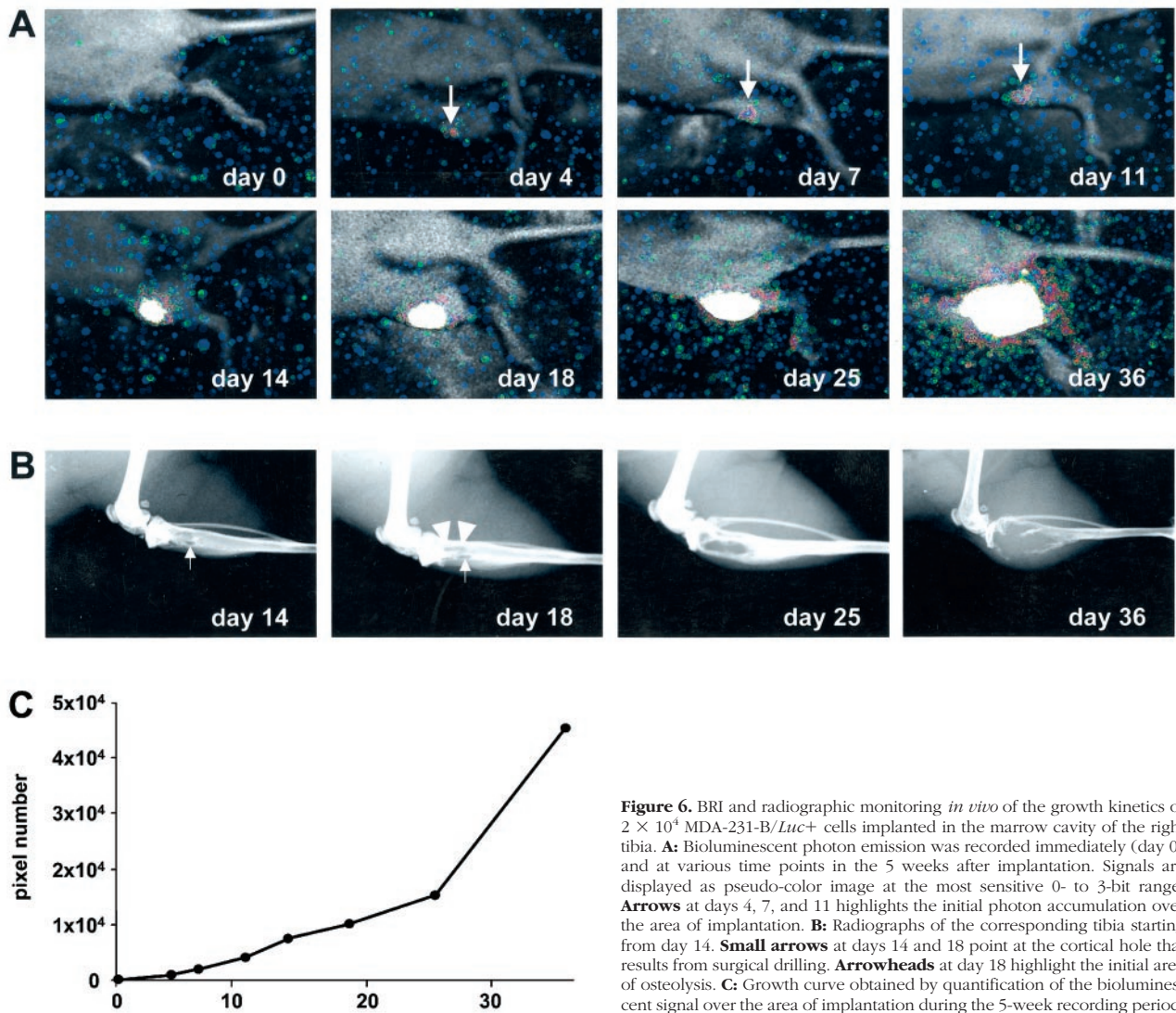
Figure 6. BRI and radiographic monitoring *in vivo* of the growth kinetics of 2×10^4 MDA-231-B/*Luc+* cells implanted in the marrow cavity of the right tibia. **A:** Bioluminescent photon emission was recorded immediately (day 0) and at various time points in the 5 weeks after implantation. Signals are displayed as pseudo-color image at the most sensitive 0- to 3-bit range. **Arrows** at days 4, 7, and 11 highlights the initial photon accumulation over the area of implantation. **B:** Radiographs of the corresponding tibia starting from day 14. **Small arrows** at days 14 and 18 point at the cortical hole that results from surgical drilling. **Arrowheads** at day 18 highlight the initial area of osteolysis. **C:** Growth curve obtained by quantification of the bioluminescent signal over the area of implantation during the 5-week recording period.

local interactions between cancer cells and the organ-specific microenvironment.[24]

All mice inoculated with the MDA-231-B subclone by intracardiac injection showed bone metastases, whereas only one-fourth of them showed soft tissue metastases, as detected by BRI. Thus the MDA-231-B possesses a higher bone-seeking capacity than the parental MDA-231 cell line, shown to induce bone metastases with lower incidence, but with a twofold higher potential to metastasize to soft tissues.[20] This modified profile of organ distribution of metastases resembles very closely that already reported for another MDA-231 subclone similarly derived from a bone metastasis.[25] In contrast, none of the animals injected intravenously with the MDA-231-B subclone developed either bone or soft tissue metastases. This seems to indicate that the cells are completely cleared by the lung already during the first passage through its circulation, further supporting the rationale for the intracardiac inoculation, as stated in the original description of the method.[11] The absence of metastatic growth in the lung after intravenous injection and the

remarkable potential to metastasize to bone marrow after intracardiac inoculation may suggest that the MDA-231-B subclone has acquired a growth advantage specific for the bone marrow microenvironment. Bone metastases induced by parental MDA-231 cells, when compared to brain and lung metastases, show increased expression of parathyroid hormone-related protein (PTH-rP),[20,25] macrophage colony stimulating factor (M-CSF), and vascular endothelial growth factor (VEGF)-A, -B, and -C.[20] All of these are bone-resorbing or angiogenic cytokines and they may represent the molecular basis for the enhanced osteotropism of bone-seeking clones derived from cancer cell lines.[20,25,26]

When compared to the conventional radiographic detection of osteolytic and/or osteosclerotic lesions, BRI offers the important advantage of detecting tumor growth in the marrow cavity much before development of radiologically evident osteolytic and/or osteosclerotic lesions. The early detection is explained by the fact that BRI detects directly tumor burden long before it reaches a critical size able to induce modifications of the local bone

remodeling relevant enough to be recognized by radiography. As a consequence, the number of metastatic sites detected by BRI largely exceeds those identified by conventional radiography. It derives a gain in statistical significance and a reduction in the number of animals needed for each experimental group.

Radiography could not detect in any of the animals an osteolytic lesion that did not show also bioluminescent activity. Furthermore, a decline of bioluminescent activity of the already developed metastases was never observed. Taken together, these observations indicate that luciferase expression *in vivo*, under nonselective conditions, was stable throughout the entire experimental period.

BRI could easily image *in vivo* a bone metastatic lesion that at the end-point histological analysis resulted in a tumor of ~0.5-mm^3 volume, corresponding to $\approx 1.7 \times 10^4$ cells. A similar number of cells could be detected when inoculated directly into the bone marrow cavity. Considering that during the time elapsed between first detection (day 33 after intracardiac injection of cancer cells) and analysis *ex vivo* (day 38) the spontaneous metastatic lesion has grown, it is likely that BRI can detect bone metastatic growth of even smaller size. Nevertheless, BRI could detect a discrete signal from 1×10^4 and 0.1×10^4 cancer cells implanted intramuscularly and subcutaneously, respectively, clearly indicating that intensity of the signal detected by BRI is a function of the tissue composition and depth of the bioluminescent source. This is possibly because of light scattering and quenching by tissue components such as hemoglobin.[16,27]

Polymerase chain reaction-based methods also allow sensitive detection and quantification of cancer cell burden in bone/bone marrow.[20,28,29] However, being methods *ex vivo*, they have severe limitations. First, in temporal studies several animal groups need to be sacrificed at different time points. Second, the bone sample is randomly selected and its size necessarily small and inevitably subject to sampling bias. Thus, large numbers of animals per group are needed to reach statistical significance. Third, these methods require disruption of the tissue samples. This precludes the possibility to perform parallel histology-based and gene expression analyses on the same bone sample. In contrast, BRI allows detailed anatomical information, continuous monitoring, and precise quantification of bone metastatic growth *in vivo*; consistent reduction in the number of experimental animals; and opportunity to perform end-point histological, immunohistological, and gene expression analyses guided to the bone(s) specifically affected by metastatic disease.

A similar method of whole-body reporter gene imaging able to visualize *in vivo* experimental metastases to bone and soft tissues has been reported.[17] This method utilizes GFP, instead of luciferase, as reporter gene. A possible concern regarding the use of GFP as reporter gene in whole-body imaging is the autofluorescence generated in animal tissues by external light excitation.[16,17] This background fluorescence may decrease the sensitivity of detection and, thus, delay early identification of bone metastatic foci. The GFP-based whole-body imaging could visualize a bone metastatic lesion of ~0.96 mm

in diameter at best.[17] At this tumor size the cancer cells may have already induced osteolytic and/or osteosclerotic lesions sufficient to be recognized by radiography. However, the sensitivity of GFP-reporter external imaging was not compared to radiography, and no histological proof of the presence and histomorphometric measurement of the size of the bone metastases were given.[17]

All carcinomas, both primary and secondary, when they reach the size of 2 to 3 mm^3 depend on angiogenesis for further growth.[14,15] The ability of BRI to detect externally bone metastatic foci of even smaller size is extremely relevant in view of the necessity to investigate the preangiogenic and periangiogenic phases of metastatic growth.

The model of intracardiac injection of *Luc*-transfected cancer cells coupled to BRI detection and continuous monitoring *in vivo* of bone metastases will facilitate studies on the molecular mechanisms involved in early stages of metastatic disease (minimal residual disease) and the development of innovative therapeutic strategies.

References

1. Boring CC, Squires TS, Tong T: Cancer statistics, 1993. CA Cancer J Clin 1993, 43:7–26
2. Jaffe HL: Tumors metastatic to the skeleton. Tumors and Tumorous Conditions of the Bone and Joints. Edited by HL Jaffe. Philadelphia, Lea and Febiger, 1968, pp 589–618
3. Drew M, Dickinson RB: Osseous complications of malignancy. Clinical Cancer Medicine, Treatment Tactics. Edited by J Lokich. Boston, Hall, 1980, pp 97–124
4. Thalmann G, Anezinis P, Devoll R, Farach-Carson C, Chung LWK: Experimental approaches to skeletal metastasis of human prostate cancer. Principles and Practices of Genitourinary Oncology. Edited by D Raghavan, HI Scher, SA Leibel, PH Lange. Philadelphia, Lippincott-Raven, 1997, pp 409–416
5. Willis RA: The spread of tumors in the human body. London, Butterworth, 1973, pp 229–250
6. Braun S, Pantel K: Micrometastatic bone marrow involvement: detection and prognostic significance. Med Oncol 1999, 16:154–165
7. McDonnell CO, Hill ADK, McNamara DA, Walsh TN, Bouchier-Hayes DJ: Tumor micrometastases: the influence of angiogenesis. Eur J Surg Oncol 2000, 26:105–115
8. Hirsch-Ginsberg C: Detection of minimal residual disease: relevance for diagnosis and treatment of human malignancies. Annu Rev Med 1998, 49:111–122
9. Kostler WJ, Brodowicz T, Hejna M, Wiltschke C, Zielinski CC: Detection of minimal residual disease in patients with cancer: a review of techniques, clinical implications, and emerging therapeutic consequences. Cancer Detect Prev 2000, 24:376–403
10. Klein CA: The biology and analysis of single disseminated tumour cells. Trends Cell Biol 2000, 10:489–493
11. Arguello F, Baggs RB, Frantz CN: A murine model of experimental metastasis to bone and bone marrow. Cancer Res 1988, 48:6876–6881
12. Yoneda T, Sasaki A, Mundy GR: Osteolytic bone disease in breast cancer. Breast Cancer Res Treat 1994, 32:73–84
13. Yoneda T: Cellular and molecular basis of preferential metastasis of breast cancer to bone. J Orthop Sci 2000, 5:75–81
14. Hanahan D, Folkman J: Patterns and emerging mechanisms of the angiogenic switch during tumorigenesis. Cell 1996, 86:353–364

15. Carmeliet P, Jain RK: Angiogenesis in cancer and other diseases. Nature 2000, 407:249–257

16. Contag CH, Jenkins D, Contag PR, Negrin RS: Use of reporter genes for optical measurements of neoplastic disease in vivo. Neoplasia 2000, 2:41–52

17. Yang M, Baranov E, Jiang P, Sun FX, Li XM, Li L, Hasegawa S, Bouvet M, Al-Tuwaijri M, Chishima T, Shimada H, Moossa AR, Penman S, Hoffman RM: Whole-body optical imaging of green fluorescent protein-expressing tumors and metastases. Proc Natl Acad Sci USA 2000, 97:1206–1211

18. Edinger M, Sweeny TJ, Tucker AA, Olomu AB, Negrin RS, Contag CH: Noninvasive assessment of tumor cell proliferation in animal models. Neoplasia 1999, 1:303–310

19. Cailleau R, Yong R, Olive M, Reeves WJ: Breast tumor cell lines from pleural effusions. J Natl Cancer Inst 1974, 53:661–674

20. van der Pluijm G, Sijmons B, Vloedgraven H, Deckers M, Papapoulos S, Löwik C: Monitoring metastatic behavior of human tumor cells in mice with species-specific polymerase chain reaction: elevated expression of angiogenesis and bone resorption stimulators by breast cancer in bone metastases. J Bone Miner Res 2001, 16:1077–1091

21. Nordeen SK: Luciferase reporter gene vectors for analysis of promoters and enhancers. Biotechniques 1988, 6:454–458

22. Wang CW, Chang YW: A model for osseous metastasis of human breast cancer established by intrafemur injection of MDA-MB-435 cells in nude mice. Anticancer Res 1997, 17:2471–2474

23. Basse P, Hokland P, Heron I, Hokland M: Fate of tumor cells injected into the left ventricle of heart in Balb/c mice: role of natural killer cells. J Natl Cancer Inst 1988, 80:657–665

24. Fidler IJ: Critical determinants of cancer metastasis: rationale for therapy. Cancer Chemother Pharmacol 1999, 43:S3–S10

25. Yoneda T, Williams PJ, Hiraga T, Niewolna M, Nishimura R: A bone-seeking clone exhibits different biological properties from the MDA-MB-231 parental human breast cancer cells and a brain-seeking clone in vivo and in vitro. J Bone Miner Res 2001, 16:1486–1495

26. Koeneman KS, Yeung F, Chung LWK: Osteomimetic properties of prostate cancer cells: a hypothesis supporting the predilection of prostate cancer metastasis and growth in the bone environment. Prostate 1999, 39:246–261

27. Colin M: Haemoglobin interferes with the ex vivo luciferase luminescence assay: consequence for detection of luciferase reporter gene expression in vivo. Gene Ther 2000, 7:1333–1336

28. Negrin RS, Blume KG: The use of the polymerase chain reaction for the detection of minimal residual disease. Blood 1991, 78:255–258

29. Sung V, Cattell DA, Bueno JM, Murray A, Zwiebel JA, Aaron AD, Thompson EW: Human breast cancer cell metastasis to long bone and soft organs of nude mice: a quantitative assay. Clin Exp Metastasis 1997, 15:173–183